

Time Resolved Fano Resonances

Marlene Wickenhauser,¹ Joachim Burgdörfer,¹ Ferenc Krausz,^{2,3,4} and Markus Drescher⁵

¹*Institute for Theoretical Physics, Vienna University of Technology, A-1040 Vienna, Austria*

²*Department für Physik, Ludwig-Maximilians-Universität München, 85748 Garching, Germany*

³*Institute for Photonics, Vienna University of Technology, A-1040 Vienna, Austria*

⁴*Max-Planck-Institute for Quantum Optics, D-85748 Garching, Germany*

⁵*Faculty of Physics, University of Bielefeld, D-33615 Bielefeld, Germany*

(Received 7 May 2004; published 18 January 2005)

Recent advances in the generation of sub-fs extreme ultraviolet pulses and attosecond metrology have opened up the possibility to trace the time evolution of electronic wave packets inside atoms in pump-probe experiments. We investigate the feasibility of observing the buildup of a Fano resonance in the time domain by attosecond streaking techniques. A time-resolved resonance is initialized by a sub-fs extreme ultraviolet-pump pulse in the presence of a synchronized phase-controlled probe laser pulse. The time evolution of the coherent superposition of resonant state and continuum is mapped onto a modulation of the electron spectrum as a function of the time delay between pump and probe pulse. (super-)Coster-Kronig transitions with lifetimes of ~ 400 asec are identified as prime candidates.

DOI: 10.1103/PhysRevLett.94.023002

PACS numbers: 32.80.Dz, 32.80.Fb, 32.80.Hd

Following the time evolution of a coherently excited wave packet in real time in a pump-probe setting has become possible with the advent of femtosecond laser pulses. The time resolution suffices to map out the vibronic motion of molecules [1], the phonon dynamics in solids [2], and the electronic dynamics in Rydberg states [3]. Resolving the dynamics of electrons in atoms near the ground states or in inner shells has remained, however, a major challenge. Only very recently, extreme ultraviolet (XUV) pulses with durations of a few hundred attoseconds have become available [4]. The time structure is comparable to the time scale of electronic processes in inner shells of atoms and opens up the perspective to perform time-resolved measurements of the electronic dynamics in atoms [5]. In a first proof of principle experiment, a 900 asec XUV pulse was used to induce a nonresonant core hole excitation in krypton which relaxes by Auger decay. Its lifetime of about 8 fs was measured in the time domain by probing the “arrival time” of the Auger electron in the continuum with the envelope of a synchronized fs laser probe pulse and was found to be in accord with the spectroscopic data [6]. More recently, the time evolution of primary electron emission could be measured with a resolution of 100 asec by using the controlled oscillation of the electric field of few-cycle probe laser light [7]. The technique has been dubbed attosecond streak camera [8]. In this Letter we study how more complex coherent dynamics proceeding on a time scale comparable to that of the duration of the sub-fs XUV excitation can be probed by this novel technique and to what extent novel information may be obtained from such time-domain studies as compared to conventional time-integral measurements.

A prototype case for the coherent dynamics in a nonstationary system is the excitation of a Fano resonance. Fano line shapes are a ubiquitous feature of resonance

scattering when the continuum can be accessed both directly and by way of a quasibound state embedded in the continuum (autoionization). Fano line shapes have been observed in the spectrum of time-integral measurements in a variety of phenomena including photoabsorption in atoms [9,10], electron and neutron scattering [11,12], Raman scattering [13], photoabsorption in quantum well structures [14], scanning tunneling microscopy [15], and ballistic transport through quantum dots (“artificial atoms”) [16]. Interest in analyzing Fano profiles is stimulated by their high sensitivity to the details of the scattering process, in particular, to the degree of transient coherence in the scattering system. Observing the nonstationary coherent dynamics by exciting a Fano resonance using an ultrashort pulse has, so far, not yet been attempted.

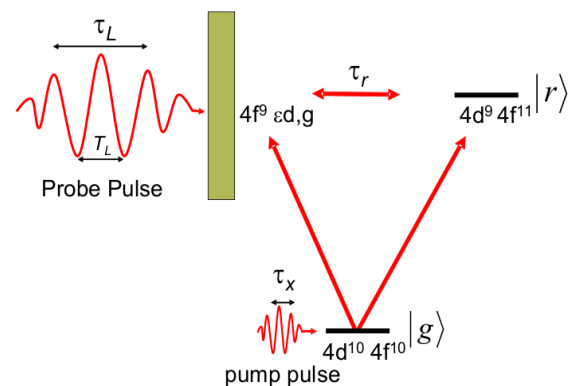


FIG. 1 (color online). Time-resolved excited Fano resonance, schematically. Excitation by the ultrashort pump pulse (duration τ_x) opens two interfering paths from the ground state to the continuum. Arrival in the continuum is monitored by the probe laser pulse with period $T_L = 2\pi/\omega_L$ and length τ_L . The indicated electronic configurations correspond to the Dy atom.

Interferences between different coherently excited autoionizing resonances have, however, been observed indirectly in ion-atom collisions [17]. In a pump-probe approach, the duration of the pump pulse τ_X should be shorter than the lifetime τ_r of the resonant state $|r\rangle$ embedded in the continuum $|E\rangle$. With the availability of sub-fs XUV pulses with $\tau_X \approx 250$ asec and the attosecond streak camera technique, observation of coherent excitation of inner shells appears to be within reach. In the following, we present first results of our exploratory study for a generic model system tailored with atomic systems such as the lanthanides [18] in mind.

The atomic model system we consider consists of a ground state $|g\rangle$ and a resonant state $|r\rangle$ embedded in a structureless continuum $|E\rangle$ (Fig. 1). The resonant state lies above the ionization threshold of the field-free Hamiltonian. We study its time evolution under the influence of a sub-fs high-frequency low-intensity pump pulse which initializes the Fano resonance and a low-frequency, moderate-intensity probe pulse. The Hamiltonian

$$H(t) = H_0 + V + H_X(t) + H_L(t), \quad (1)$$

consists of the atomic Hamiltonian $H_a = H_0 + V$, where H_0 is the single configuration Hamiltonian and V is the residual configuration interaction. $H_X(t) = -dF_X(t)$ and $H_L(t) = -dF_L(t)$ are the dipolar interactions with the XUV pump field $F_X(t)$ and probe laser field $F_L(t)$ ($d = -\sum_i z_i$ is the dipole operator). All dependences on angular momentum and emission angles are suppressed and the emission direction is assumed to be along the direction of the polarization of the laser field. In the absence of the coupling V between the resonant state and the continuum, $|r\rangle$ would be a bound eigenstate of H_0 , $H_0|r\rangle = E_r|r\rangle$. V couples the resonant state $|r\rangle$ and the near-degenerate continuum $|E\rangle$. The diagonalization of H_a in terms of stationary states $|\Psi_E\rangle$ is the cornerstone of Fano's treatment of the autoionization process [10,19]. These Fano states $|\Psi_E\rangle$ can be written as

$$|\Psi_E\rangle = \frac{\sin[\Delta(E)]}{\pi V_E} |\phi_E\rangle - \cos[\Delta(E)] |E\rangle, \quad (2)$$

with

$$|\phi_E\rangle = |r\rangle + PP \int dE' \frac{V_{E'}}{E - E'} |E'\rangle, \quad (3)$$

and $\Delta(E)$ the mixing angle. The coupling matrix element between continuum and resonance is denoted by $V_E = \langle E|V|r\rangle$ and PP denotes the principal part value of the integral. Near the resonance energy E_r , the emission spectrum can be parametrized as

$$P(E) = \frac{|q + \epsilon|^2}{1 + \epsilon^2}, \quad (4)$$

with $\epsilon = \frac{E - E_r - \delta E}{\Gamma/2}$, where $\Gamma = 1/\tau_r$ and δE is a shift of the resonance position due to the coupling to the continuum. If V_E is only weakly energy dependent near the resonance, this shift is small and can be neglected

[10,20]. Equation (4) describes an asymptotic spectral profile with Fano parameter

$$q = \frac{\langle \phi_{E_r} | T | g \rangle}{\pi V_{E_r} \langle E_r | T | g \rangle}, \quad (5)$$

where T is the transition operator for the excitation. q represents the ratio of the transition amplitude from the ground state to the resonant state $|\phi_{E_r}\rangle$ to the amplitude of the excitation of the structureless continuum. Our starting point for treating time-dependent Fano resonances generated by ultrashort pulses is the solution of the time-dependent rather than the stationary Schrödinger equation, i.e.,

$$|\psi(t)\rangle = \hat{T} e^{-i \int_{-\infty}^t H(t') dt'} |g\rangle. \quad (6)$$

The goal is to calculate the time- and energy-differential ionization probability $P(E, t) = |\langle E | \psi(t) \rangle|^2$. Its asymptotic limit $P(E) = \lim_{t \rightarrow \infty} P(E, t)$ converges to the time-integral emission spectrum of a Fano resonance in the limit where the influence of the probe laser pulse can be neglected. We solve Eq. (6) under a number of simplifying assumptions. The weak XUV pulse is treated in first-order perturbation theory and we neglect all other couplings except those involving the ground state. Consequently, Eq. (6) can be reduced to

$$|\psi(t)\rangle = -i \int_{-\infty}^t dt' \tilde{U}(t, t') H_X(t') |g\rangle_{t'}, \quad (7)$$

where the time-evolution operator \tilde{U} is governed by H_a and $H_L(t)$. Its equation of motion can be written as

$$\tilde{U}(t, t') = U_L(t, t') - i \int_{t'}^t dt'' U_L(t, t'') V \tilde{U}(t'', t') \quad (8)$$

with

$$U_L(t, t') = e^{-i \int_{t'}^t [H_0 + H_L(t'')] dt''}. \quad (9)$$

Equation (8) provides a convenient starting point for approximately incorporating the effect of the probe laser. Since its intensity is only moderate ($I_L \approx 10^{12}$ W/cm²) and its one-photon energy is of the order of the outer shell ionization energy, its effect on the deeply bound level $|g\rangle$ can be safely neglected. However, the effect of the probe laser must be taken into account nonperturbatively for the final continuum states $|E\rangle$, for which we involve the strong-field approximation [21]. Accordingly, U_L in Eq. (9) will be replaced by the Volkov propagator, U_V , of free electrons

$$U_V(t, t') |E\rangle = e^{-i \Phi_V(E, t, t')} |E(t, t')\rangle, \quad (10)$$

where $\Phi_V(E, t, t')$ is the Volkov phase, $\Phi_V(E, t, t') = \int_{t'}^t dt'' E(t'', t')$, with $E(t'', t') = [p_E + A(t'')/c - A(t')/c]^2/2$. The resonant state is assumed to be either unaffected or only weakly perturbed which can be taken into account by a complex dynamical Stark shift $\Delta E_S^c(t)$ that includes both a real energy shift ΔE_S as well as a damping due to coupling to other states outside the subspace of the Fano resonance. Consequently, \tilde{U} inside the integral on the right-hand side of (8) can be replaced by the

propagator for Fano states, possibly modified for dynamical Stark shifts, $U_F(t, t') = \exp\{-i \int_{t'}^t dt'' [H_0 + V + |r\rangle\Delta E_S^c(t'')\langle r|]\}$. With these approximations, the time-energy-differential ionization amplitude becomes

$$\begin{aligned} \langle E|\psi(t)\rangle = & -i \int_{-\infty}^t dt' e^{i\Phi_V(E, t', t)} \dot{a}_{E(t', t)}(t') - \int_{-\infty}^t dt' \int_{t'}^t dt'' \int d\tilde{E} e^{i\Phi_V(E, t'', t)} V_{E(t'', t)} \langle r|U_F(t'', t')|\tilde{E}\rangle \dot{a}_{\tilde{E}}(t') \\ & - \int_{-\infty}^t dt' \int_{t'}^t dt'' e^{i\Phi_V(E, t'', t)} V_{E(t'', t)} \langle r|U_F(t'', t')|r\rangle \dot{a}_r(t'), \end{aligned} \quad (11)$$

with $\dot{a}_E(t) = \langle E|H_X(t)|g\rangle_t$ and $\dot{a}_r(t) = \langle r|H_X(t)|g\rangle_t$. The three terms in Eq. (11) represent different coherent pathways to the continuum final state $|E\rangle$: the first two terms describe the direct excitation resulting from transition from the ground state to the Volkov continuum in the absence of the resonance (first term) modified by a correction term due to interactions with the resonance (second term). The latter signifies virtual transitions from the continuum to the resonance and back to the continuum. The third term describes indirect transitions to the continuum via the resonant state $|r\rangle$. The present treatment is somewhat complementary to the analysis of laser excitation of autoionizing resonances [22] in which the resonant coupling between the ground state and the autoionizing resonance is treated nonperturbatively within the framework of the rotating wave approximation.

It is instructive to analyze first the temporal evolution of the Fano resonance, $P(E, t)$ in the absence of a probe pulse. Figure 2 shows the case of the evolution of a typical asymmetric Fano resonance in the time-integral limit [$q = 1$ in Eq. (5)]. In view of anticipated experimental investigations of super-Coster-Kronig transitions in the 4d giant resonances of the lanthanides [18], we chose a lifetime of the autoionizing resonance $\tau_r = (2\pi|V_E|^2)^{-1} = 400$ asec, an XUV pulse of duration $\tau_X \approx 250$ asec, and excitation energy of $\hbar\omega_X = 150$ eV. The probe laser pulse has a mean photon energy $\hbar\omega_L = 1.6$ eV corresponding to a cycle period $T_L = 2.6$ fs. For $t \lesssim \tau_r$ the broad spectral distribution reflects the width of the XUV pump pulse

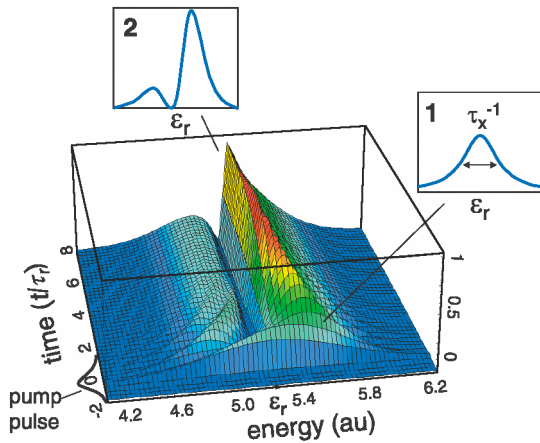


FIG. 2 (color). Time-dependent ionization probability $P(E, t)$ as a function of energy and time. Inset 1: spectral distribution at short times $t \leq \tau_r$. Inset 2: spectral distribution in the scattering limit $t \rightarrow \infty$ for $q = 1$.

$\approx \tau_X^{-1}$ (inset 1). For $t \gtrsim \tau_r$ the wave packet representing this spectral distribution acquires an internal structure due to the coupling to the quasibound level $|r\rangle$. As a result, the destructive interference due to the transient coupling to the resonance starts to “burn a hole” into the energy distribution at times $t/\tau_r \gtrsim 1$. Finally, in the limit $t \rightarrow \infty$ the spectral distribution converges to that of an asymmetric Fano resonance (inset 2). Clearly, as this ultrafast rearrangement process happens on the time scale of the lifetime of a Coster-Kronig resonance, direct observation of $P(E, t)$ is out of reach. However, pump-probe experiments provide the key to retrieve real-time information about such fast processes by correlating the wave packet with a probing light field. The pump pulse $F_X(t) = \cos(\omega_X t)f_X(t)$ initializes the coherent excitation and a delayed probe laser pulse $F_L(t) = \cos[\omega_L(t + \Delta t)]f_L(t)$ probes the population of the continuum states. We assume both envelope functions f_X and f_L to be Gaussians where the duration of the probe pulse is long compared to that of the pump $\tau_L \gg \tau_X$ (in current experiments $\tau_L \geq 5$ fs). The field of the probe pulse modifies the energy and momentum distribution of the emitted electrons which depends on the time delay Δt . Consequently, the observed time-integral spectrum will depend on Δt , $P(E, t \rightarrow \infty) = P_{\Delta t}(E)$ and thereby provides time-differential information. Two limiting cases can be distinguished [6,23]. If the lifetime is much shorter than the period of the probe laser pulse, $\tau_r \ll T_L$ the energy spectrum fluctuates due to the oscillations of the vector potential $\vec{A}(t)$ entering the canonical momentum and thus resembles the behavior of a classical particle in an oscillating electric field. In the opposite limit of long lifetime compared to the period of the probe pulse, $\tau_r \gg T_L$, the quantized nature of the interaction of the electron with the radiation field is retained and energy shifts occur in multiples of the photon energy $\hbar\omega_L$ giving rise to spectral sidebands. Figure 3 displays typical simulated spectra $P_{\Delta t}(E)$ as a function of pump-probe delay. The resulting signal depends on three different time scales: the lifetime of the resonance, τ_r , the duration of the pump pulse, τ_X and the period, T_L , of the probe pulse. We present results for two different lifetimes of the resonance: $\tau_r = 400$ asec corresponding to the giant resonance in Dy and, for comparison, a significantly larger lifetime of 2.5 fs. A rich variety of spectral features as a function of delay time can be observed. The key point is that these intricate features in $P_{\Delta t}(E)$ appear only when all three time scales τ_X , τ_r , and T_L are comparable to each other. Figure 3(a) shows the spectrum for the case of a window resonance

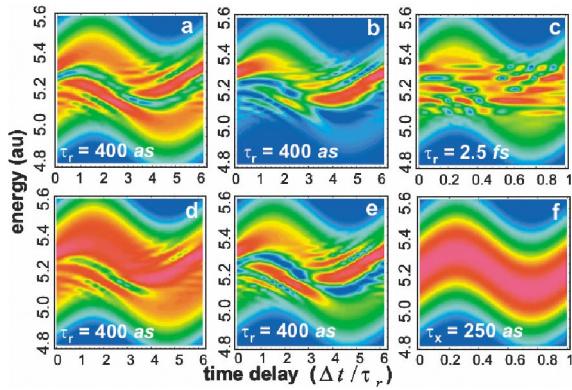


FIG. 3 (color). $P_{\Delta t}(E)$ as a function of the time delay between pump and probe pulse and observed in the direction of the polarization of the probe laser pulse. (a) Direct ionization with the resonant excitation suppressed ($q = 0$), (b)–(c) autoionizing resonance with both pathways open ($q = 2.2$) for different τ_r , (d)–(e) complex Fano parameters with $q = 2.2e^{i\pi/4}$ and $q = 2.2e^{-i\pi/4}$, respectively, and (f) ionization in the absence of a resonance ($\dot{a}_r = 0$, $V_E = 0$).

($\dot{a}_r = q = 0$). In Figs. 3(b) and 3(c) the spectra for a generic autoionization process with interfering open pathways for the direct and the resonant channels [all three terms in Eq. (11) contribute] are shown. For short lifetimes, an asymmetric Fano profile with the q value of the Dy resonance ($q = 2.2$) is still recognizable unlike the case of longer lifetimes. Remarkably, in Fig. 3(c) complementary time and spectral features are simultaneously present. Both the resonant and the direct ionization channels contribute to the population of the sidebands.

One extension of this approach is the investigation of complex Fano parameters. While for systems with time-reversal symmetry q is real, in systems with broken time-reversal symmetry [24,25] due to the presence of decoherence and time-dependent fields, q may take on complex values. One remarkable feature of the time-integral spectral distribution $P(E)$ is that it is invariant under complex conjugation $q \rightarrow q^*$; i.e., the phase angle cannot be uniquely determined. The time-resolved spectrum, instead, $P_{\Delta t}(E)$, is found to be sensitive to this phase angle. Figures 3(d) and 3(e) display the attosecond streak spectra for the same parameters as in Fig. 3(b), however, for complex Fano parameters with phase $\pm\pi/4$. For comparison, Fig. 3(f) shows the direct ionization in the absence of a resonance. Another extension is the coherent excitation of several closely spaced resonances [18]. This leads to a more complex streaking image from which information on the energy spacing between the resonances can be extracted. Clearly, for strong streaking probe pulses the direct even-order multiphoton coupling between interfering channels may strongly perturb the resonances such that resonance parameters may no longer be easily determined.

In summary, we have presented first evidence for the feasibility to observe time-resolved Fano resonances in

inner atomic shells by utilizing the recently demonstrated attosecond streak camera technique. The evolution of the nonstationary wave packet results in a rich variety of structures in the experimental observable, the time-delay spectral distribution $P_{\Delta t}(E)$. Coster-Kronig-type processes within the parameter range explored in this Letter are expected to become accessible to experimental observation in atomic vapors of metal atoms, e.g., the lanthanide group. The method holds the promise of identifying and quantifying coherent as well as incoherent pathways to ionization. Similarly, observation of time-resolved Fano resonances in doped quantum dots employing THz radiation should be possible.

The authors thank O. Smirnova, V. Yakovlev, and A. Scrinzi for helpful discussions. This work has been supported by (FWF-SFB016, Austria).

-
- [1] M. Dantus, R.M. Bowman, and A.H. Zewail, *Nature (London)* **343**, 737 (1990).
 - [2] M. Hase *et al.*, *Phys. Rev. B* **58**, 5448 (1998).
 - [3] J. A. Yeazell and J. C. R. Stroud, *Phys. Rev. Lett.* **60**, 1494 (1988); C. Raman *et al.*, *ibid.* **76**, 2436 (1996).
 - [4] M. Hentschel *et al.*, *Nature (London)* **414**, 509 (2001).
 - [5] C. A. Nicolaides, T. Mercouris, and Y. Komninos, *J. Phys. B* **35**, L271 (2002); T. Mercouris, Y. Komninos, and C. A. Nicolaides, *Phys. Rev. A* **69**, 032502 (2004).
 - [6] M. Drescher *et al.*, *Nature (London)* **419**, 803 (2002).
 - [7] R. Kienberger *et al.*, *Nature (London)* **427**, 817 (2004).
 - [8] J. Itatani *et al.*, *Phys. Rev. Lett.* **88**, 173903 (2002).
 - [9] H. Beutler, *Z. Phys.* **93**, 177 (1935).
 - [10] U. Fano, *Phys. Rev.* **124**, 1866 (1961).
 - [11] R. K. Adair, C. K. Bockelman, and R. E. Peterson, *Phys. Rev.* **76**, 308 (1949).
 - [12] J. Simpson and U. Fano, *Phys. Rev. Lett.* **11**, 158 (1963).
 - [13] F. Cerdeira, T. A. Fjeldly, and M. Cardona, *Phys. Rev. B* **8**, 4734 (1973).
 - [14] J. Faist *et al.*, *Nature (London)* **390**, 589 (1997).
 - [15] V. Madhavan *et al.*, *Science* **280**, 567 (1998).
 - [16] J. Göres *et al.*, *Phys. Rev. B* **62**, 2188 (2000).
 - [17] J. Burgdörfer and R. Morgenstern, *Phys. Rev. A* **38**, 5520 (1988).
 - [18] C. Dzionk *et al.*, *Phys. Rev. Lett.* **62**, 878 (1988).
 - [19] U. Fano, *Nuovo Cimento* **12**, 156 (1935).
 - [20] U. Eichmann, T. F. Gallagher, and R. M. Konik, *Phys. Rev. Lett.* **90**, 233004 (2003).
 - [21] L. Keldysh, *Sov. Phys. JETP* **20**, 1307 (1965); F. H. M. Faisal, *J. Phys. B* **6**, L89 (1973); H. R. Reiss, *Phys. Rev. A* **22**, 1786 (1980).
 - [22] P. Lambropoulos and P. Zoller, *Phys. Rev. A* **24**, 379 (1981).
 - [23] O. Smirnova, V. S. Yakovlev, and A. Scrinzi, *Phys. Rev. Lett.* **91**, 253001 (2003).
 - [24] K. Kobayashi *et al.*, *Phys. Rev. B* **68**, 235304 (2003).
 - [25] A. A. Clerk, X. Waintal, and P. W. Brouwer, *Phys. Rev. Lett.* **86**, 4636 (2001).